

Chapter 11

The Indian Ocean

We now turn to the Indian Ocean, which is in several respects very different from the Pacific Ocean. The most striking difference is the seasonal reversal of the monsoon winds and its effects on the ocean currents in the northern hemisphere. The absence of a temperate and polar region north of the equator is another peculiarity with far-reaching consequences for the circulation and hydrology.

None of the leading oceanographic research nations shares its coastlines with the Indian Ocean. Few research vessels entered it, fewer still spent much time in it. The Indian Ocean is the only ocean where due to lack of data the truly magnificent textbook of Sverdrup *et al.* (1942) missed a major water mass - the Australasian Mediterranean Water - completely. The situation did not change until only thirty years ago, when over 40 research vessels from 25 nations participated in the International Indian Ocean Expedition (IIOE) during 1962 - 1965. Its data were compiled and interpreted in an atlas (Wyrтки, 1971, reprinted 1988) which remains the major reference for Indian Ocean research. Nevertheless, important ideas did not exist or were not clearly expressed when the atlas was prepared, and the hydrography of the Indian Ocean still requires much study before a clear picture will emerge. Long-term current meter moorings were not deployed until two decades ago, notably during the INDEX campaign of 1976 - 1979; until then, the study of Indian Ocean dynamics was restricted to the analysis of ship drift data and did not reach below the surface layer.

Bottom topography

The Indian Ocean is the smallest of all oceans (including the Southern Ocean). It has a north-south extent of 9600 km from Antarctica to the inner Bay of Bengal and spans 7800 km in east-west direction between southern Africa and western Australia. Without its southern ocean part it covers an area of $48 \cdot 10^6$ km². If the southern ocean part is included, the area increases to $74.1 \cdot 10^6$ km². The only large shelf area is the Northwest Australian Shelf, a region of strong tidal dissipation. It is part of the large expanse of continental shelf between Australia and south-east Asia that continues as the Timor and Arafura Seas and the Gulf of Carpentaria; however, these latter regions are considered part of the Pacific Ocean. The Northwest Australian Shelf itself is insufficient in size to have much impact on the mean depth of the Indian Ocean, which with 3800 m is between that of the Pacific and Atlantic Oceans. Most basins show depths well below 5000 m; in the east, the *Wharton Basin* exceeds 6000 m depth. The *Arabian Sea* reaches depths below 3000 m over most of its area, while the depth in the *Bay of Bengal* decreases gradually from 4000 m south of Sri Lanka to 2000 m and less at 18°N.

Three mediterranean seas influence the hydrographic properties of Indian Ocean water masses. The Persian Gulf is the smallest of the three; with a mean depth of 25 m, a maximum depth of only 90 m, and a sill which rises barely above the mean depth its impact is not felt much beyond the Gulf of Oman. The Red Sea is a very deep basin with maximum depths around 2740 m and a mean depth near 490 m; its sill depth is about 110 m. The Australasian Mediterranean Sea, a series of very deep basins with depths exceeding 7400 m, communicates with the Indian Ocean through various passages between the Indonesian islands where the depth is in the range 1100 - 1500 m.

Two ridge systems run through the Indian Ocean in a roughly meridional direction, dividing it into three parts of about equal size (Figure 11.1). The *Central Indian Ridge* between the western and central part is a northward extension of the interoceanic ridge system (Figure 8.1) and connects with the ridge systems of the Atlantic and Pacific Oceans at a bifurcation point in the south. Similar to the East Pacific Rise and Mid-Atlantic Ridge it is a broad structure which rises consistently above 4000 m; again and again it reaches above 3000 m (in the region of the Mascarene Plateau it rises high enough to influence upper ocean currents), but numerous fractures and depressions make the blockage for water flow incomplete at that level. The Eastern Indian or *Ninety East Ridge* stretches in nearly perfect north-south orientation from the Andaman Islands to 33°S. It is much narrower and less fractured than the other ridges. South of 10°S it reaches the 3000 m level consistently and the 2000 m level frequently. South of 30°S it rises above 1500 m and merges with the *Southeast Indian Ridge* (a continuation of the Central Indian Ridge) at the 4000 m level. The *Broken Plateau* branches off to the east near 30°S, also reaching above 1500 m. North of 10°S the Ninety East Ridge shows occasional gaps in the 3000 m contour. The passages are apparently deeper than the merging depth of the ridge systems in the south and therefore provide a bottom water entry point for the Central Indian Basin in the northeast.

In contrast to the central and eastern parts of the Indian Ocean which are dominated by single basins of large meridional extent, the western part is subdivided by secondary ridges and the island of Madagascar into a series of smaller deep basins. The Arabian Basin is closed in the south by the merger of the *Carlsberg*, *Central Indian*, and *Chagos-Laccadive Ridges*. The merger region shows extremely complicated topography with multiple fracture zones; but the closure is complete somewhere near the 3500 m level, somewhat higher than the deepest passage in the Owen Fracture Zone. As a consequence the bottom water entry point for the Arabian Basin is also found in the north rather than in the south.

The wind regime

Monsoonal climate dominates the northern Indian Ocean, and its effects are felt far into the subtropics of the southern hemisphere. Annual mean distributions of atmospheric and oceanic parameters are therefore of only limited use. Instead, we define two mean states and discuss both separately. The information is again contained in Figs 1.2 - 1.4. A summary of the monsoon cycle is given in Figure 11.2. An introductory but comprehensive account of monsoon meteorology is given by Fein and Stephens (1987).

The *Northeast* or *Winter Monsoon* determines the climate of the northern Indian Ocean during the northern hemisphere winter (December - March). It is characterized by high pressure over the Asian land mass and northeasterly winds over the tropics and northern subtropics. The situation resembles the annual mean wind circulation over the Pacific Ocean, except that the Intertropical Convergence Zone (ITCZ) and the Doldrums are located south of the equator (near 5°S) rather than north. The wind over the northern Indian Ocean represents the Trades, but because of its seasonality it is known as the Northeast Monsoon. (The word monsoon is derived from the Arabic, meaning seasonally reversing winds.) Since most of the air pressure gradient is retained behind the Tibetan Plateau, air pressure gradients over the ocean are small. This protects the ocean from the full force of the winds blowing off the Mongolian high pressure region and results in a wind of moderate strength, comparable to the Pacific Northeast Trades which are also relatively weak at this time of

The Southwest Monsoon, as this wind is called in the northern hemisphere, is the continuation of the southern hemisphere Trades, which between 10 and 20°S are stronger, during this time of year, than anywhere else in the world. The Southwest Monsoon skirts the low over Pakistan to deposit rain on the Himalayas, thus bringing with it the monsoon rains and floods that are so crucial to Asian agriculture.

The position of the ITCZ over the ocean changes little between the seasons, but during the Southwest Monsoon frequent disturbances break away from it to settle south of the Himalayas, bringing with them most of the season's rain. Winds at the equator change direction but remain weak throughout the year. Because of their meridional orientation the associated Ekman transport does not develop a divergence at the equator. There is therefore no equatorial upwelling in the Indian Ocean. Strong equatorial downwelling occurs during the transition months (May and November) when the winds turn eastward at the equator, producing Ekman transport convergence.

Conditions for coastal upwelling are also markedly different in the Indian Ocean. Along the eastern coastline, where the most important upwelling regions of the Pacific and Atlantic Oceans are found, winds favourable for upwelling along the Australian coast are weak during the Northeast Monsoon season and absent during the Southwest Monsoon season. A small upwelling region can be expected in the latter season along the coast of Java. But the strongest upwelling of the Indian Ocean occurs along its western coastline when the Southwest Monsoon produces strong Ekman transport away from the coasts of Somalia and Arabia.

We saw in Chapter 4 that the Sverdrup relation, which compares circulation patterns derived from annual mean integrated steric height and annual mean wind stress, gives very good agreement in the Indian Ocean despite the seasonal reversals of the monsoon winds. It is therefore instructive to look at the annual mean atmospheric circulation over the Indian Ocean as well. The southern hemisphere Trades stand out as particularly strong, in the annual mean, when compared with the other oceans. As we have seen, the larger contribution to this comes from the Summer Monsoon season. The stronger winds of this season dominate the annual mean in the northern Indian Ocean as well. This produces a net southwesterly stress over the northwestern Indian Ocean and in particular along the East African coast. Mean winds in the northeast and along the equator are weak and westerly.

The integrated flow

We begin the comparison between the depth-integrated flow (Figs 4.4 - 4.7) and the observed surface circulation (Figure 11.3) with the southern Indian Ocean which does not experience monsoonal winds. The Sverdrup stream function (Figure 4.7) shows a particularly strong subtropical gyre, a result of large wind stress curl between the annual mean Trades and Westerlies (Figure 1.4). South of 10°S and away from the Australian coast the pattern agrees well with the observations. Both show the South Equatorial Current being fed by the throughflow of Pacific water through the Indonesian seas and strengthening westward. The bifurcation east of Madagascar and again near the African coast is also seen in the Sverdrup flow, as is the joining of the Mozambique and East Madagascar Currents into the Agulhas Current. Furthermore, the Sverdrup relation implies net southward flow across 10°S in response to strong negative wind stress curl; this generates the eastward flowing Equatorial Countercurrent north of 10°S as its source of supply. To the best of our

Significant discrepancies between the Sverdrup circulation and observations are seen in the Agulhas Current extension region, for reasons discussed in Chapter 4, and in the Leeuwin Current. The net depth-averaged flow along the Australian coast is in fact very close to that given by the Sverdrup circulation; but the shallow Leeuwin Current is accompanied by an undercurrent of nearly equal transport (to be discussed below), and the surface circulation is therefore not representative for the depth-averaged flow.

In contrast, the annual mean flow in the northern Indian Ocean is almost featureless, both in the Sverdrup circulation maps and in observations. The stream function map does not show a single streamline for the northern hemisphere, so any mean circulation that does develop must be weaker than 10 Sv (the contour interval used for Figure 4.7). This is, of course, a somewhat theoretical result since it represents the mean of two strong monsoonal current systems. The annual mean is still of use when it comes to the calculation of heat fluxes between the hemispheres, and we shall come back to this in Chapter 18. But in a discussion of monsoonal surface currents the Sverdrup relation has its limits, and we now turn to a description based on current and hydrographic observations.

During the Northeast Monsoon season the current system resembles closely those of the Pacific and Atlantic Oceans. The subtropical gyre dominates the southern hemisphere. For a long time it was believed that eastward flow in the south is achieved by the Circumpolar Current. Following the recent discovery of the South Atlantic Current as a distinct element of the south Atlantic subtropical gyre (Chapter 14), Stramma (1992) showed the existence of a similar South Indian Ocean Current north of the Circumpolar Current. The current follows the northern flank of the Subtropical Front, carrying some 60 Sv in the upper 1000 m southeast of Africa and gradually releasing its waters into the gyre. Southwest of Australia its transport is reduced to about 10 Sv. Zonal flow immediately south of the Subtropical Front is usually weak, indicating that the South Indian Ocean and the Circumpolar Currents are two distinct features of the circulation.

The subtropical gyre of the northern hemisphere is not well-defined; most of the water carried in the North Equatorial Current returns east with the Equatorial Countercurrent near 5°S, leaving little net transport for the weak currents in the northern Indian Ocean. The Equatorial Countercurrent continues into the South Java Current, which during this season feeds its waters into the Indonesian seas and southward into the South Equatorial Current. Currents flow in the opposite direction north of 10°S during the Southwest Monsoon season, when the South Equatorial Current intensifies and feeds part of its flow into the Somali Current, the western boundary current of the anticyclonic circulation that develops in the northern hemisphere. The North Equatorial Current disappears, and the Equatorial Countercurrent becomes absorbed into the Southwest Monsoon Current. Its broad eastward flow dominates the northern Indian Ocean.

A feature of the circulation which is independent of the monsoon cycle is the strong separation of the northern and southern hemisphere flow fields along the ITCZ east of 60°E. Little flow crosses the Doldrums east of the western boundary current. The semi-annual reversal of the intense flow across the ITCZ along the east African coast north of 10°N has been well documented during the last two decades. However, it is obvious that at least some of the water that enters the northern hemisphere from June to October in the west must leave it during that season. Likewise, at least some of the water that is withdrawn during December to April has to enter it somewhere in the east during these months. Our knowledge of the circulation near Java is, however, incomplete, and the details of the mass balance on seasonal time scales are a topic for the future.

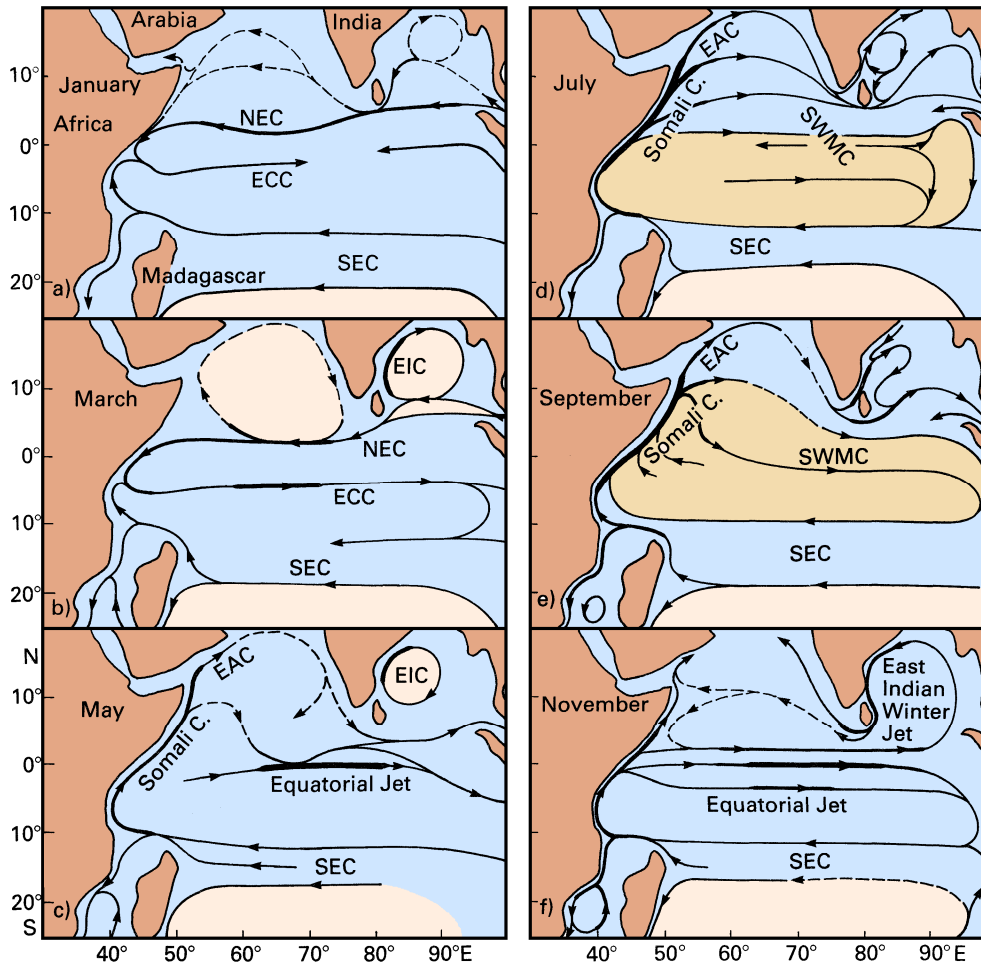


Fig. 11.4. Surface currents in the northern Indian Ocean as derived from ship drift data. SEC: South Equatorial Current, NEC: North Equatorial Current, ECC: Equatorial Countercurrent, SWMC: Southwest Monsoon Current, EAC: East Arabian Current, EIC: East Indian Current. Adapted from Cutler and Swallow (1984).

When the Southwest Monsoon is fully established during July and September, the entire region north of 5°S is dominated by the eastward flow of the *Southwest Monsoon Current*, the only exception being a narrow strip along the equator in July to which we shall return in a moment. Velocities in the Southwest Monsoon Current are generally close to $0.2 - 0.3 \text{ m s}^{-1}$, but an acceleration to $0.5 - 1.0 \text{ m s}^{-1}$ occurs south and southeast of Sri Lanka. The South Equatorial Current expands slightly towards north, reaching 6°S in September. The transition before the onset of the Northeast Monsoon (Figure 11.4f) is again characterized by the Equatorial Jet. Concentrating all eastward flow in a 600 km wide

layers above the thermocline. Winds at the equator are generally light, the meridional wind component being dominated by the annual monsoon cycle. The zonal wind component, on the other hand, shows westerly winds during the transition periods and exerts a strong semi-annual signal on the ocean. The associated change of current direction produces semi-annual variations in thermocline depth and sea level (Figure 11.6). The 20°C isotherm rises off Africa and falls off Sumatra during periods of eastward flow, indicating a net transport of 20 Sv in the equatorial band. The same transport in the opposite direction occurs during periods of westward flow when the 20°C isotherm rises off Sumatra and falls off Africa. The associated zonal slope of the thermocline finds its mirror image (as expressed in our Rule 1a of chapter 3) in the slope of the sea surface, as indicated by the sea level at Sumatra.

Figure 11.5 suggests a direct relationship between the zonal current and the zonal wind. However, the current is not purely wind-driven. An array of current meter moorings was deployed along the equator between 48°E and 62°E during INDEX (1979 - 1980), with instruments at 250 m, 500 m, and 750 m depth. The semi-annual current reversal occurred at all depths, much deeper than could be explained by direct wind forcing (Luyten and Roemmich, 1982). It appears that the wind reversal in the west is only the triggering mechanism for a wave phenomenon peculiar to the equatorial region known as a Kelvin wave. The same process is responsible for interannual climate variations in the equatorial Pacific Ocean which will be discussed in detail in Chapter 19. We therefore leave the explanation of Kelvin waves to that chapter and note here only the essence of the process, which is as follows. The arrival of westerly winds in the west lifts the thermocline up near the African coast. The resulting bulge in the thermocline travels eastward, accompanied by strong eastward flow, until it reaches Sumatra. Thus, eastward flow does not occur simultaneously but propagates along the equator. This explains why we find both eastward and westward flow at the equator on occasions, as in Figs. 11.4a and d.

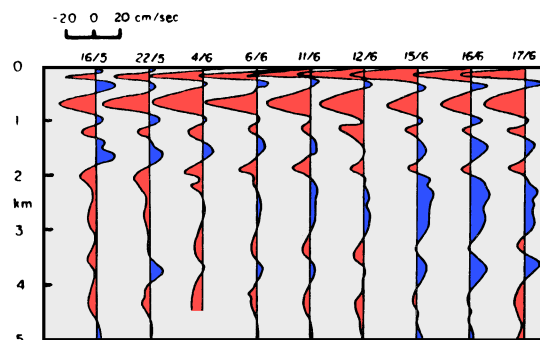


Fig. 11.7. Eastward components of velocity on the equator at 53°E. After Luyten and Swallow (1976).

The limited information available on subsurface flow near the equator indicates a complicated and unique current regime. Observations with profiling current meters show that the currents reach to great depth with only slightly reduced velocities (Figure 11.7). Several layers of alternate flow direction were found, with velocities reaching 0.12 m s^{-1} at 4000 m depth. The uppermost layer of westward flow near 200 m depth is commonly referred to as the *Equatorial Undercurrent*; but it is obvious that westward transport occurs at

September coastal temperatures are lowered by 5°C and more (Figure 11.8). The fact that the upwelling is embedded in a western boundary current reduces its effectiveness for primary production - the swift current removes much of the additional biomass from the system before it can be utilized. Compared to upwelling regions in the Pacific and Atlantic Ocean, zooplankton levels in the Arabian Sea upwelling are much less exceptional. Nevertheless, an abundance of sea birds off the Arabian coast during the upwelling period indicates that it is sufficient to support a significant marine resource.

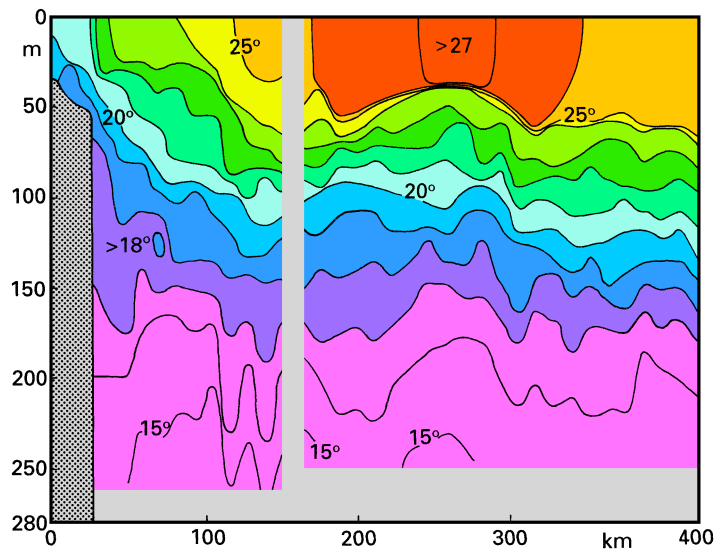


Fig. 11.8. A temperature section across the Arabian upwelling region during July 1983, from the Kuria Muria Islands (18°N) towards southeast. The break in the isotherm slope about 150 km from the coast separates the coastal upwelling to the left from the Ekman suction region to the right. After Currie *et al.* (1973).

An increase of zooplankton biomass associated with a drop in sea surface temperatures reminiscent of upwelling has also been documented for the western Indian shelf during the Southwest Monsoon season (Figure 11.9). Since the Southwest Monsoon cannot drive the surface waters offshore on that coast, the reasons for the increased productivity must be found elsewhere. Most likely the phenomenon is related to nearshore advection of river water associated with the monsoon rains and not to the oceanic circulation.

The circulation in the Bay of Bengal is characterized by anticyclonic flow during most months and strong cyclonic flow during November. In January currents are weak and variable. In the west, the *East Indian Current* strengthens as the Northeast Monsoon becomes stronger, exceeding 0.5 m s^{-1} in March (Figure 11.4b) and remaining strong ($0.7 - 1.0 \text{ m s}^{-1}$) until May/June. Throughout this time the current runs into the wind, apparently as an extension of the North Equatorial Current. The fact that it persists during May when flow south of the Bay turns eastward is remarkable and still requires an explanation. During the Southwest Monsoon season currents in the entire Bay are weak and

patterns. A first path (*a* in Figure 11.10a) continues north along the west coast to return south with the Mozambique Current (*a'*). In the second path (*b*) the current flows directly west. Both paths feed into the Agulhas Current (*c*), going through a cyclonic loop (*d*) on their way. The third path, complete retroflexion south of Madagascar (*c'*), cuts the East Madagascar Current off from the Agulhas Current; it is rarely followed by drifting buoys but occasionally seen in satellite data (Figure 11.10b).

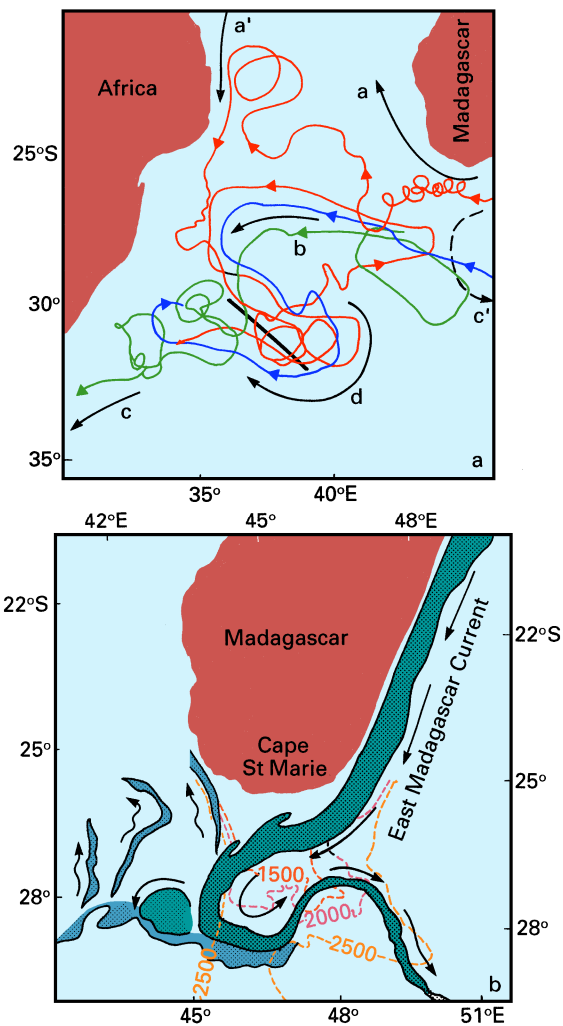


Fig. 11.10. Paths of the East Madagascar Current extension. (a) from tracks of satellite-tracked drifters, (b) from a satellite image of sea surface temperature on 13 June 1984. The warm core of the East Madagascar Current is indicated by dark shading. Light shading indicates intermediate water temperatures. The heavy line in (a) is the location of the section shown in Fig. 11.11. See the text for the meaning of letters in (a). After Lutjeharms *et al.* (1981), Gründlingh (1987) and Lutjeharms (1988).

The contribution of the *Mozambique Current* to the Agulhas Current is comparatively small. Although southward transport along the African shelf through Mozambique Strait was estimated at 30 Sv near 15°S, the Mozambique Current contributed only 6 Sv to this flow, the remaining 24 Sv coming from the northward looping East Madagascar Current (Zahn, 1984); in other words, the net southward transport near 15°S was only 6 Sv.

prediction of Sverdrup theory which indicates a continuation of the current toward South America (Figs. 4.4 - 4.7). The reason for the striking departure from Sverdrup dynamics is that the current enters the Atlantic Ocean as a free jet and develops instabilities accompanied by eddy shedding, in a manner similar to the generation of East Australian Current eddies: The retroflection loop moves westward until its western part pinches off and the loop retreats to its most eastern position. (The two positions are indicated in Figure 11.13a by the crowding of front locations near 15°E and 19°E.) Most eddies are ejected into the Benguela Current and drift away toward northwest; in Figure 11.13c two eddies are seen by the depression of the thermocline in their centres (as explained with Figure 3.3). The eddies are among the most energetic in the world ocean and are believed to have life spans of many years. The associated transport of Indian Central Water into the Atlantic Ocean is an important element in the recirculation of North Atlantic Deep Water (see Chapter 7). Observations show that net transfer of water between the two oceans is westward in the thermocline (above 1500 m) but eastward underneath. Estimates for the time-averaged transfer of thermocline water from Agulhas Current eddies range from 5 to 15 Sv.

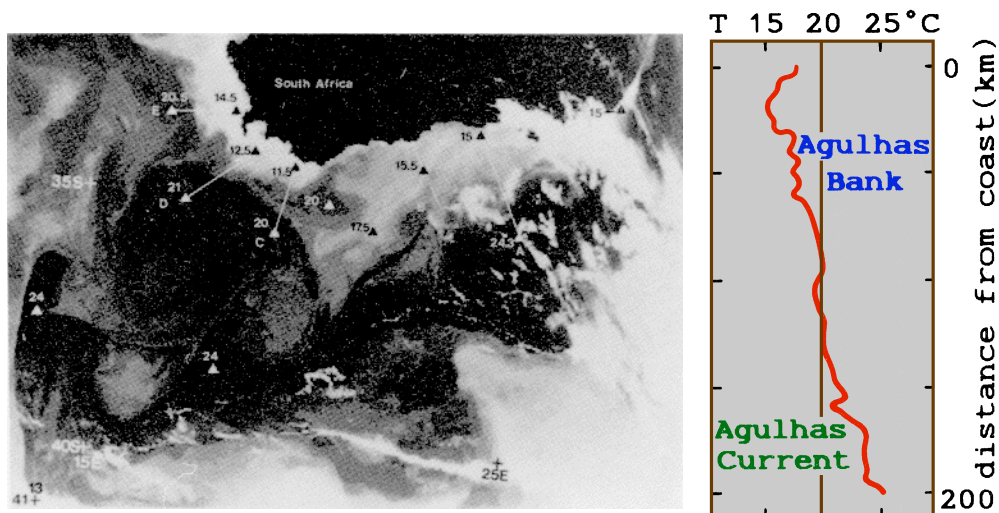


Fig. 11.12. Upwelling over the Agulhas Bank induced by the Agulhas Current. (a) Satellite image of sea surface temperature (dark is warm; small light patches are clouds. Numbers next to triangles are temperature in °C), (b) Temperature section along the track labelled A in (a). From Walker (1986).

Near 25°E the Agulhas Plateau which reaches above 2500 m depth causes a northward excursion and further instability in the path of the retroflection current. The feature is seen in the frontal positions of Figure 11.13a; it was observed as early as 1899 when the steamer *Waikato* broke down on the Agulhas Bank and drifted in the current for 100 days; it rounded the Agulhas Plateau, looped through two eddies, and drifted eastward, reaching 65°E after a journey of 5000 km.

Winds near southern Africa are westerly to southwesterly throughout the year, bringing cold unsaturated maritime air over the Agulhas Current system. Unlike the Gulf Stream and Kuroshio the Agulhas Current therefore loses heat during all seasons. On average annual net heat loss amounts to 75 W m^{-2} , less than half of the values found in the northern hemisphere. A unique aspect of the region is that the Mozambique, East Madagascar, and Agulhas Currents all run against the prevailing wind direction during the Southwest Monsoon season. This produces a steepening of the wind waves. Further south the current runs into the mature swell of the Southern Ocean. The resulting steepening of the swell produces some of the most dangerous waves of the world ocean; with wave heights of 20 m and more and a steepness that can cause ordinary wind waves of the open ocean to turn into breakers they are capable of inflicting severe damage on the largest vessels.

North of 10°S the East African Coastal or *Zanzibar Current* flows northward, fed by the northern branch of the South Equatorial Current. Because of its permanent character it is well resolved in the vertically integrated flow (Figure 4.7). During the Northeast Monsoon season it runs against light winds and is opposed by the southward flowing Somali Current. The point where northward and southward flows meet at the surface moves from 1°N at the beginning of the season to 4°S during the February peak, when the Zanzibar Current is at its weakest. Soon after the peak it starts moving north again, reaching the equator by early April. Throughout this period the current feeds into the Equatorial Countercurrent. Below the surface flow the Zanzibar Current flows northward across the equator at all times, taking the form of an undercurrent under the southward flowing Somali Current during the Northwest Monsoon season (Figure 11.14). During the Southwest Monsoon season the strength of the Zanzibar Current increases considerably; INDEX observations from April/May 1979 show it with speeds of 2.0 m s^{-1} and a transport of 15 Sv. The current now feeds the northward flowing Somali Current; some consider it part of the Somali Current during these months.

Southward flow in the *Somali Current* during the Northeast Monsoon is limited to the region south of 10°N . It first occurs in early December south of 5°N and expands rapidly to 10°N in January (Figure 11.4a) with velocities of $0.7 - 1.0 \text{ m s}^{-1}$. In March the southward flow contracts again to 4°N , until the surface flow reverses in April. During the Southwest Monsoon the Somali Current develops into an intense jet with extreme velocities; INDEX observations gave surface speeds of 2.0 m s^{-1} for mid-May and 3.5 m s^{-1} and more for June.

South of 5°N the Somali Current is extremely shallow; below 150 m depth southward flow is maintained throughout the year (Figure 11.15). Further north the jet deepens, eventually embracing the permanent thermocline. The current structure on the equator is extremely complex and shows layering similar to the equatorial flow further east (Figure 11.7) but oriented northward-southward.

The period of northward flow can be divided into two phases of different dynamics. During the transition in May, flow in the Equatorial Jet is eastward, and westward flow develops only slowly during the following two months. From the point of view of mass continuity there is not much need for a strong western boundary current until the monsoon reaches its peak in August, and the Somali Current is first established as a response to the wind reversal along the African coast. Winds are southerly but light in late April and May and strengthen abruptly in late May or June. This drives northward flow across the equator; but the flow turns offshore near 3°N , and a coastal upwelling regime develops between 3°N and 10°N . Figure 11.16a displays this division into two separate northward flows in the sea

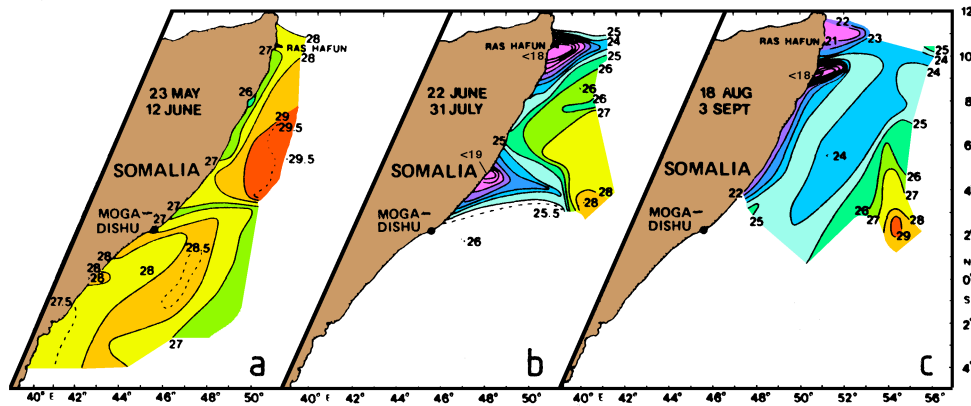


Fig. 11.16. Development of the Somali Current during the onset of the Southwest Monsoon as seen in the sea surface temperature during 1979. (a) Advection of warm water south of 3°N and coastal upwelling north of 3°N, (b) two gyres with upwelling regions near 4°N (minimum temperature <19°C) and Ras Hafun (minimum temperature <18°C), (c) continuous northward flow and upwelling near Ras Hafun (minimum temperature <17°C). From Evans and Brown (1981).

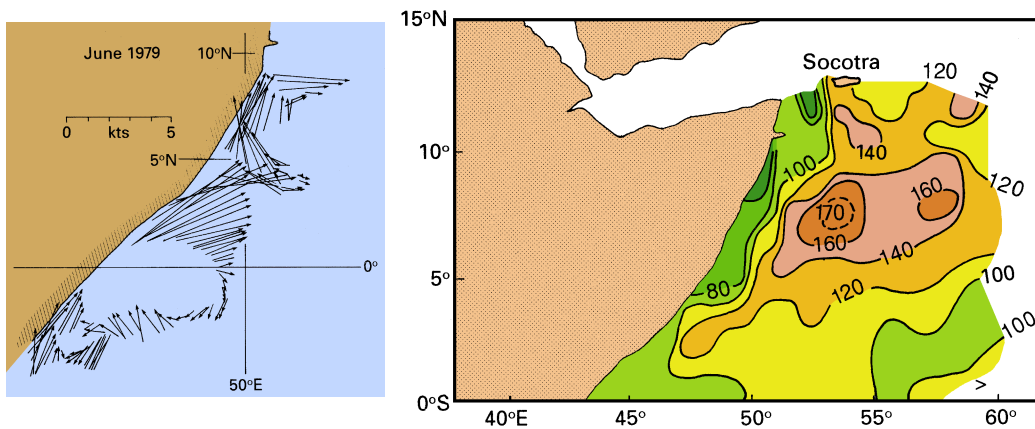


Fig. 11.17. The two-gyre phase of the Somali Current. (a) Surface currents in June 1979 along the track of *Discovery*, (b) the northern gyre as seen in the mean depth of 20°C isotherm (m) during June. This eddy is often called the “Great Whirl”. From Swallow and Fieux (1982) and Bruce *et al.* (1980).

Eastern boundary currents

The eastern boundary of the tropical Indian Ocean is different from the Atlantic and Pacific eastern boundaries in several respects. First, the mean temperature and salinity stratification is less developed than off Peru and West Africa, so when upwelling occurs it

heat loss. The process is self-perpetuating, as southward flow is accompanied by surface cooling, and surface cooling produces southward flow.

As mentioned before, the dynamics of the currents along the western Indian shelf during the Northeast Monsoon are similar to those of the Leeuwin Current. In the northern hemisphere case the large alongshore steric height gradient is the result of differences in water temperature and salinity produced by the monsoon winds combined with seasonal cooling.

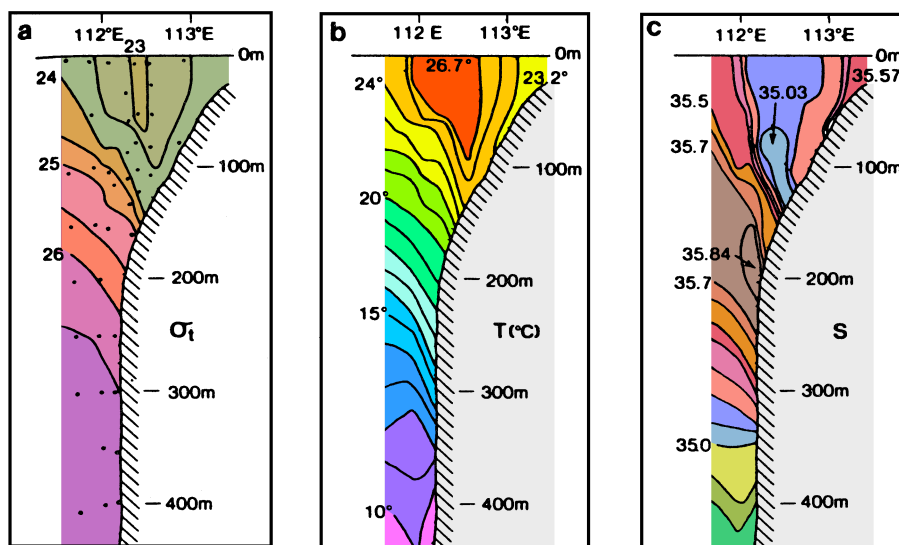


Fig. 11.18. Hydrographic properties in the Leeuwin Current near 25°S. (a) Density, (b) temperature (°C), (c) salinity. Note the deep mixed layer produced by convective cooling between 112°E and 113°E. From Thompson (1984).

The annual mean transport of the Leeuwin Current is estimated at 5 Sv, with average current velocities of $0.1 - 0.2 \text{ m s}^{-1}$. However, the intensity and southward extent of the current vary strongly with the seasons, in response to variations in the southerly wind and perhaps also the alongshore pressure gradient. The southerly wind is weakest in May. At this time the Leeuwin Current passes round Cape Leeuwin at speeds of up to 1.5 m s^{-1} and enters the Great Australian Bight. The associated advection of warm low salinity water produces a distinct seasonal cycle in the water properties along the western Australian coast (Figure 11.19) and hydrographic fronts on the offshore and inshore edges of the current (Figure 11.20). Eddies produced by the strong current shear across the fronts are clearly visible in satellite images of sea surface temperature (Figure 11.21).